

24. RARE-EARTH ELEMENTS, $^{87}\text{Sr}/^{86}\text{Sr}$, AND $^{143}\text{Nd}/^{144}\text{Nd}$ MANTLE SOURCE VARIATIONS¹

M. L. Rideout and J.-G. Schilling, Graduate School of Oceanography, University of Rhode Island²

ABSTRACT

We report 48 analyses of rare-earth elements (REE) and 15 $^{143}\text{Nd}/^{144}\text{Nd}$ and $^{87}\text{Sr}/^{86}\text{Sr}$ analyses for basalts from the eight holes drilled during Leg 82. Discrete and distinct REE patterns and $^{143}\text{Nd}/^{144}\text{Nd}$ ratios characterize the eight holes, with little variation observed downhole except in Holes 561 and 558, thus suggesting dominantly long-term temporal and large-scale spatial variations in the mantle source of these basalts beneath the Mid-Atlantic Ridge over the last 35 Ma of its spreading activity. There is a good inverse correlation between $^{143}\text{Nd}/^{144}\text{Nd}$ and $(\text{La}/\text{Sm})_{\text{EF}}$ with one exception in Hole 558 (approximately 35 Ma), the latter suggesting a recent (35 Ma) light REE depletion event, perhaps caused by dynamic or fractional melting. Short-term temporal and small-scale spatial mantle source variability is also evident in Hole 561 (approximately 18 Ma), which has rapid fluctuations in REE patterns and $^{143}\text{Nd}/^{144}\text{Nd}$ ratios (suggesting rapid transfer of magma from the time of melting) and is evidence contrary to the presence of a well-mixed magma chamber at this particular site and time.

The mantle source variations noted can be interpreted within two extreme models. The first model invokes a convecting mantle depleted in large ion lithophile elements (LILE) and containing lumps (or veins) of LILE-enriched material of various shapes and sizes, passively and randomly distributed throughout. A second more restrictive model considers the interaction of fixed mantle plumes and the LILE-depleted asthenosphere flowing towards a migrating Mid-Atlantic Ridge (MAR) axis. With the exception of Hole 558 and the uncertainties of reconstructions of absolute plate movements in the region, the observed variations can be explained by two hot spots; the nearly ridge-centered Azores hot spot (plume) and another hot spot located beneath the African plate that may be affecting the source of basalts currently erupting at the MAR axis at 35°N and which, in the past, would have produced the New England chain of seamounts on the North American plate and (later) the Atlantis-Great Meteor chain on the African plate.

Basalts erupted south of the Hayes Fracture Zone have not been affected by either of these two hot spots over the last 35 Ma and appear to have been continuously derived from the LILE-depleted source. Subaxial flow downridge from the Azores plume appears to have started 9 Ma, on the basis of the southward converging V-shaped time-transgressive ridges branching from the Pico and Corves Island, or not earlier than 16 Ma, on the basis of the geochemical results. Variations within Hole 558 remains unexplained by the latter model, unless we hypothesize a third hot spot.

INTRODUCTION

DSDP Leg 82 was designed to examine in detail the spatial and the temporal extent of mantle heterogeneities in the central North Atlantic, near the topographic high of the Azores Platform. Shallow volcanic platforms, such as this one, are characterized by high $^{87}\text{Sr}/^{86}\text{Sr}$ (low $^{143}\text{Nd}/^{144}\text{Nd}$) and Pb isotope ratios and enriched in the light rare-earth elements (LREE) relative to the heavy rare-earth elements (HREE). They are significant because they are derived from a different mantle source than the source from which mid-ocean ridge basalt (MORB) depleted in the large ion lithophile elements (LILE) originates. On the basis of known geochemical variations along the present Mid-Atlantic Ridge (MAR) axis (Schilling, 1975; White and Schilling, 1978; Bougault and Treuil, 1980) and temporal variations along the FAMOUS flow line from Leg 37 (Schilling et al., 1977; Aumento and Melson, 1977), nine holes were drilled during Leg 82, eight of which yielded basalts suitable for this study (Fig. 1).

The arrangement of holes, complemented with data from DSDP Leg 37 and from dredge samples along the

present MAR axis, forms a coarse grid from which one may study (1) spatial variation along three isochrons (approximately 35 Ma, 18 Ma, from drilled basalt, and zero age from dredge sampling) and (2) temporal variations along four flow lines (Azores Platform, FAMOUS, 35°N , and south of the Hayes Fracture Zone, Fig. 1).

The important questions for which Leg 82 may provide answers are:

1. When and how did the large scale (> 800 km) geochemical gradient currently observed along the present MAR axis develop?

2. Was the Hayes Fracture Zone always a boundary between the enriched Azores mantle domain, rich in LILE and radiogenic Sr and Pb (low Nd), and the depleted MORB source?

3. Is the spike-like anomaly superimposed on the large-scale geochemical gradient and currently present on the MAR axis at 35°N accidental or permanent feature that may be related to the activity of a hot spot other than the Azores?

In order to address these questions, we report 48 rare-earth analyses and 15 isotopes ratio analyses of Sr and Nd on basalts from Leg 82.

ANALYTICAL PROCEDURES

The samples were selected on board with the following considerations to ensure that the sampling was:

1. representative of a chemical group, as defined by core logging and available on-board incompatible and major element data;

¹ Bougault, H., Cande, S. C., et al., *Init. Repts. DSDP*, 82: Washington (U.S. Govt. Printing Office).

² Addresses: (Rideout, present address) Rice University, Department of Geology, Weiss School of Natural Sciences, Post Office Box 1892, Houston, Texas 77251; (Schilling) Graduate School of Oceanography, University of Rhode Island, Narragansett Bay Campus, Kingston, Rhode Island 02882.

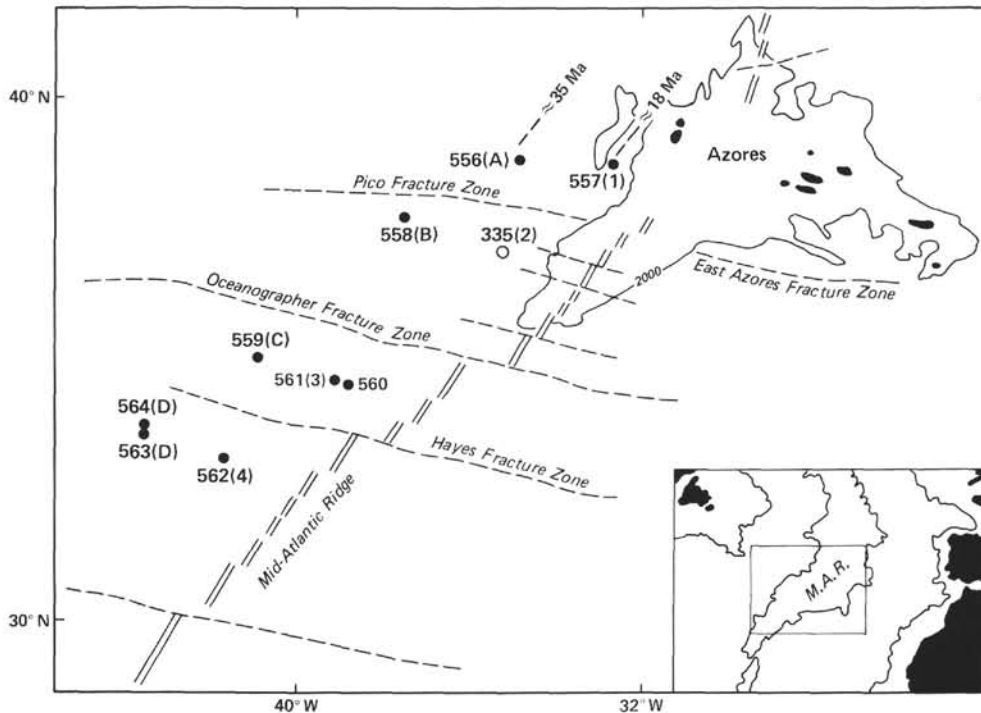


Figure 1. Map of the DSDP Leg 82 study area. Hole 335 (Leg 37), included for comparison, although it is dated at approximately 16.5 Ma. Sites along the approximately 18 Ma magnetic anomaly are represented in further diagrams by numerals, and sites along the approximately 35 Ma magnetic anomaly are represented by letters.

2. from the freshest section available, as determined by hand inspection and available geochemical and petrologic data from adjacent samples analyzed by X-ray fluorescence (XRF); and

3. frequent enough to represent adequately any chemical variations that may be present beyond what was suspected from the on-board XRF survey.

A special effort was made to take samples adjacent to XRF samples analyzed on board, wherever possible. Hand and petrologic descriptions of the basalt flows from which the samples were taken are found in the core descriptions for each site, referred to using DSDP nomenclature and numbering system.

All basalt samples were carefully broken down into small fragments; the fragments were selected to avoid calcite veinlets and alteration patches, and freshest fragments were ground into a fine powder in an agate mortar. Using approximately 0.5 g of sample powder, we analyzed 48 samples by instrumental neutron activation analysis (INAA), using essentially the same technique previously described by Schilling and Ridley (1975), slightly modified.

After INAA was completed, 15 samples were chosen for additional isotope work, based on the REE pattern identification from the concentration data. At least one sample per hole was measured, plus additional samples from Holes 558 and 561 that contained basalts with multiple REE signatures within a continuous series of basalt flows (see site chapters, Sites 558 and 561, this volume). Using approximately 0.3 g of sample powder, $^{87}\text{Sr}/^{86}\text{Sr}$ and $^{143}\text{Nd}/^{144}\text{Nd}$ isotopic ratios were determined from the same unspiked aliquot of sample. Detailed procedures for the isotopic methods used in this laboratory are described in detail in Rideout (1983) and are available on request from the authors. For $^{87}\text{Sr}/^{86}\text{Sr}$, the methods are essentially those of Hart and Brooks (1974), slightly modified to improve the separation of Ba from the rare-earth elements. Nd is then isolated from the rare-earth fraction and subsequently analyzed. Samples were run on triple filaments (Re-metal center, Ta-metal side ribbons) on a 2 VG Micro-Mass 30B mass spectrometer, with approximately 60–80 ratios collected from $^{87}\text{Sr}/^{86}\text{Sr}$ and 100–150 ratios collected for $^{143}\text{Nd}/^{144}\text{Nd}$ as a statistically representative data summation. $^{87}\text{Sr}/^{86}\text{Sr}$ data are normalized to the E & A standard of 0.70800 and $^{143}\text{Nd}/^{144}\text{Nd}$ to a BCR-1 value of 0.512650 (see Table 2 caption). The cumulative average in this laboratory for the E & A standard is 0.708031 ± 20 (2 s.d., $n = 27$) and the

BCR-1 standard is 0.512569 ± 8 (2 s.d., $n = 12$), where n is the number of analyses reported and s.d. is the standard deviation.

RESULTS

Rare-Earth Abundances: Spatial and Temporal Variations

The results of the 48 rare-earth analyses are presented in Table 1; the data are arranged by site and increasing absolute depth.

Figure 2 is a composite of the rare-earth results, plotted relative to chondrites. The patterns are grouped by hole, and the holes are arranged geographically to be similar to Figure 1. Thus, interhole variations along a vertical column represents spatial variations along the ridge axis at a particular time (approximately 35 Ma, 18 Ma, and zero age), and interhole variation along a horizontal row illustrates the temporal variation at a given point on the ridge (or temporal variation along a flow line from the spreading ridge axis). The REE patterns suggest the existence of discrete chemical groups among the holes, and in two cases within a single hole (Holes 558 and 561). Thus, in general, each site is characterized by a unique type of REE pattern (i.e., depleted, enriched, or intermediate), with only slight second-order relative concentration variations downhole. This can be interpreted as reflecting long-term (temporal) and large-scale (spatial) variations at the Mid-Atlantic Ridge axis at approximately 18 and 35 Ma. As for the two exceptions noted, Hole 561 contains multiple REE patterns, strongly enriched in LREE at the top of the hole, and suddenly changing to strongly depleted in

Table 1. Rare-earth element analyses of DSDP Leg 82 basalts.

Hole-Core-Section (piece number)	La	Ce	Nd	Sm	Eu	Tb	Dy	Yb	Lu	(La/Sm) _{EF}
556-2-1 (6B)	1.7	6.6	5.7	2.37	0.90	0.62	5.0	2.43	0.344	0.51
556-3-1 (8B)	2.8	9.5	8.1	3.64	1.28	0.77	6.6	3.64	0.499	0.55
556-4-5 (3C)	3.1	11.2	8.9	3.70	1.31	0.87	5.9	3.75	0.533	0.58
556-6-2 (2A)	2.2	9.4	7.8	3.05	1.14	0.86	5.5	3.28	0.498	0.52
556-9-2 (3c)	1.9	5.2	4.9	2.33	0.90	0.54	4.1	2.49	0.328	0.58
556-11-1 (16)	2.4	7.9	7.4	3.12	1.19	0.69	4.7	3.14	0.445	0.53
556-12-3 (5B)	1.3	4.7	4.9	1.78	0.81	0.50	3.5	2.02	0.299	0.52
556-16-2 (15)	2.5	7.9	8.1	3.01	1.18	0.72		3.39	0.493	0.59
557-111, CC	25.5	61.7	32.0	7.58	2.61	1.37	7.6	3.95	0.499	2.36
557-1-1 (10)	18.7	43.3	25.7	7.29	2.39	1.54	8.1	3.39	0.463	1.79
558-27-3 (11B)	5.9	15.8	8.8	2.79	1.03	0.62	3.7	2.23	0.301	1.47
558-28-1 (2)	5.9	14.3	9.2	2.79	1.12	0.53	3.6	2.30	0.318	1.49
558-28-2 (16)	2.4	7.8	6.0	2.54	0.92	0.59	5.0	2.60	0.354	0.66
558-30-2 (11)	10.0	22.6	13.0	3.42	1.23	0.65		2.43	0.409	2.06
558-33-1 (4)	8.6	20.8	11.8	3.07	1.17	0.58		2.17	0.326	1.97
558-33-2 (9)	8.5	19.7	10.0	2.94	1.02	0.48	3.9	2.13	0.291	2.03
558-36-3 (3A)	7.6	19.0	11.0	2.97	1.12	0.61		2.64	0.370	1.79
558-38-1 (14)	4.8	12.2	6.9	2.11	0.82	0.51	2.8	2.13	0.276	1.59
558-39-2 (3A)	4.9	11.4	7.5	2.24	0.84	0.59	3.5	2.02	0.291	1.54
559-1-4 (2)	9.6	22.0	12.3	3.63	1.33	0.85		3.22	0.441	1.85
559-6-1 (5)	8.4	21.6	11.7	3.10	1.13	0.74		2.73	0.398	1.89
559-8-3 (3)	8.8	20.0	11.3	3.39	1.29	0.68		3.11	0.472	1.81
561-111, CC	12.7	26.4	12.7	3.60	1.25	0.72	4.4	2.54	0.332	2.46
561-1-1 (2C)	11.1	23.9	11.6	3.13	1.16	0.70		2.21	0.343	2.48
561-1-1 (9A)	2.7	8.2	8.0	3.14	1.14	0.75	5.7	3.62	0.495	0.60
561-1-2 (2C)	2.6	7.8	7.7	2.94	1.24	0.88		3.57	0.504	0.62
561-2-1 (3B)	2.7	7.7	5.9	3.01	1.11	0.73	5.8	3.47	0.505	0.63
561-2-2 (2A)	2.3	8.6	7.1	3.07	1.16	0.75	5.5	3.24	0.536	0.52
561-2-3 (10A)	2.4	9.4	7.5	3.01	1.19	0.87	5.5	3.52	0.554	0.56
561-3-1 (9J)	2.3	8.4	8.2	3.06	1.18	0.89	5.7	3.47	0.509	0.54
561-3-2 (4A)	2.4	9.4	8.7	3.05	1.18	0.88	5.1	3.54	0.466	0.55
562-2-2 (1)	2.7	9.5	8.6	3.36	1.31	0.83		3.78	0.544	0.57
562-4-1 (3E)	2.9	9.1	8.5	3.54	1.28	0.80	6.9	3.61	0.516	0.57
562-7-1 (4B)	2.6	7.6	6.1	2.73	0.98	0.85		3.14	0.419	0.67
562-8-1 (2)	2.4	7.7	6.0	2.76	1.09	0.66	5.3	2.95	0.412	0.61
562-9-1 (3B)	2.6	7.5	6.3	2.53	1.06	0.72		2.87	0.442	0.71
562-10-3 (1A)	2.4	8.0	7.8	2.72	1.02	0.64	5.0	2.94	0.418	0.63
563-23-1 (2A)	1.8	6.3	5.4	2.18	0.89	0.59	4.5	2.70	0.411	0.59
563-24-2 (3A)	1.8	5.8	4.9	2.13	0.89	0.48		2.69	0.387	0.60
563-24-3 (7F)	1.6	5.8	5.3	2.14	0.83	0.56	4.6	2.56	0.335	0.54
563-25-2 (2D)	1.9	5.6	5.8	2.13	0.91	0.66	4.5	2.59	0.369	0.63
564-1-1 (2B)	3.7	11.7	10.5	3.37	1.31	0.98	5.9	3.86	0.524	0.78
564-3-4 (2)	3.5	10.3	8.8	3.24	1.31	0.84		3.57	0.505	0.76
564-5-2 (4B)	3.8	10.0	9.2	3.44	1.07	1.00	5.6	3.59	0.494	0.77
564-6-4 (2K)	3.8	9.7	8.8	3.32	1.22	0.78	5.8	3.29	0.484	0.80
564-7-2 (6B)	4.2	11.8	9.7	3.36	1.25	0.85		3.63	0.525	0.87
564-8-1 (4F)	4.2	13.2	11.2	3.47	1.34	1.00	5.7	3.68	0.549	0.84
564-9-2 (9B)	4.2	11.1	9.6	3.44	1.32	0.95		3.77	0.522	0.86

Note: All concentrations are reported in ppm. Analyses performed by instrumental neutron activation analysis, using essentially the method of Schilling and Ridley, 1975. (La/Sm)_{EF} is the La/Sm ratio normalized to chondrites. Chondrite values used for calculating enrichment factors (EF) are given in Schilling et al. (1977; 1983). For typical errors, see Schilling and Ridley, 1975.

LREE at a point downhole. No intermediate between these extremes is observed, implying that no mixing has occurred between the two "end-members." Hole 558 contains dominantly LREE-enriched patterns, but with one horizon of LREE-depleted material. In both cases, the patterns cross near the middle of the REE series.

Whereas the uniformity within a single drilled hole is interpreted as reflecting a lack of short-term geochemical variation for the interval sampled, the exceptions noted at Sites 558 and 561 would suggest the converse situation exists along the Mid-Atlantic Ridge at the time

of emplacement of the ocean basalt crust at these two sites.

Figure 2 also readily demonstrates that the spatial variations observed along the ridge at approximately 0, 18, and 35 Ma are not identical to one another. Particularly with respect to the Azores hot spot, the geochemical gradient observed along the D Ma ridge axis is not present at 18 and 35 Ma, and thus must have developed later than 18 Ma or was far more complex in the past.

Temporal variations at a given point (i.e. along a flow line) are variable from one flow line to another. South

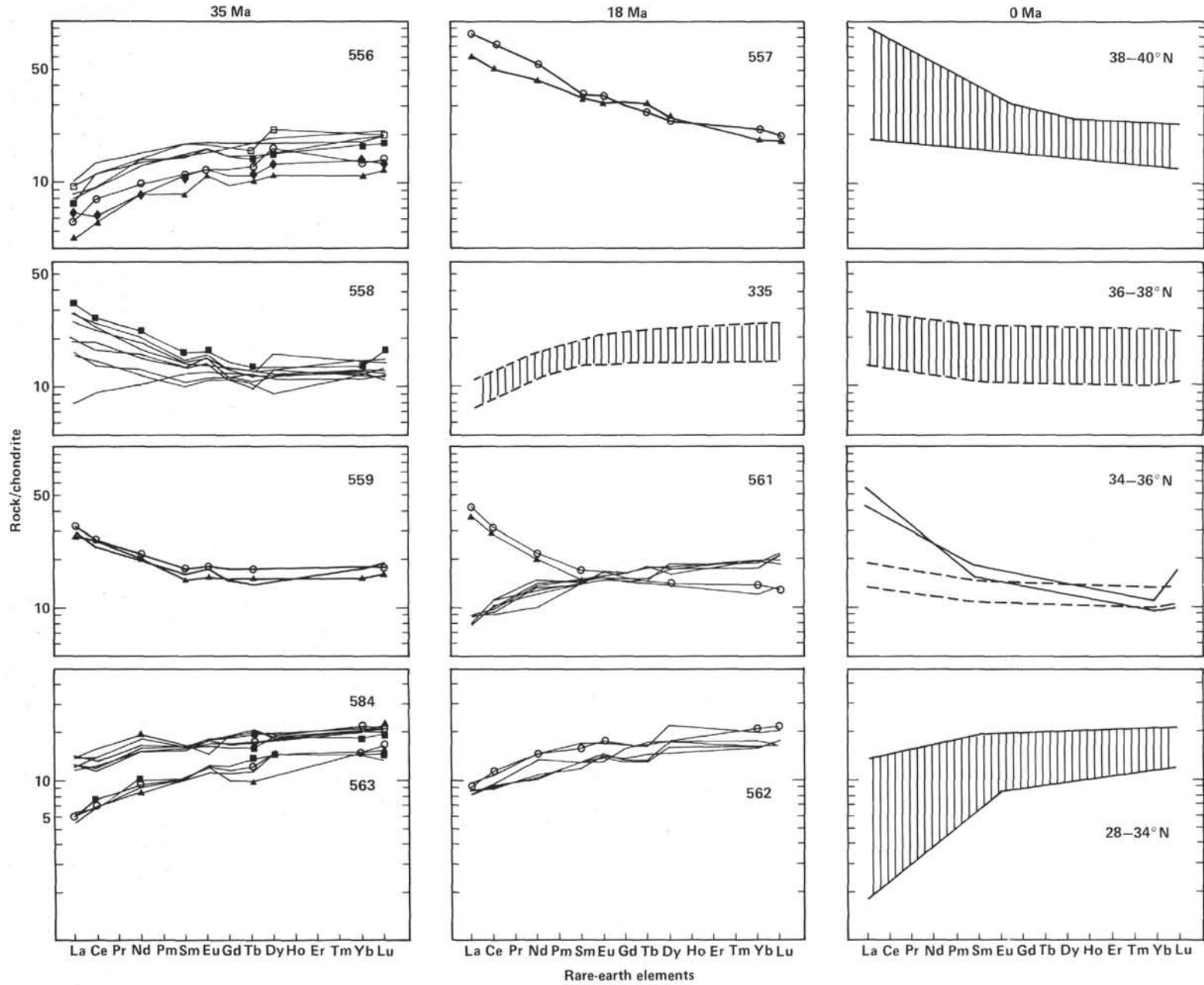


Figure 2. Composition of rare-earth abundances relative to chondrites as a function of atomic number. Data for age zero is from Schilling et al. (1983) and for Hole 335, Leg 37, from Schilling et al. (1977), O'Nions et al. (1977), and Aumento et al. (1977). Holes are grouped by isochron (columns) and spreading flow lines (rows) for direct comparison.

of the Hayes Fracture Zone, all material is uniformly depleted throughout the 35 Ma time range sampled. At the latitude of the Azores flow line, the enriched Azores anomaly was not present 35 Ma ago (Hole 556) but was present 18 Ma ago (Hole 557). Therefore, the LREE enriched anomaly must have begun at a time, t , so that $35 < t < 18$ Ma. Along the FAMOUS flow line, Schilling et al. (1977) suggested a progressive increase in LREE enrichment, from the LREE-depleted basalts at Hole 335, Leg 37 (approximately 16.5 Ma) to progressively more LREE enrichment patterns in Hole 332 (3.5 Ma) (Aumento, Melson, et al., 1977) and, at the present, in the FAMOUS region. Thus, the gradient generated by the Azores hot spot did not exist at 16.5 Ma or did not extend that far down the ridge and must have developed at a time between 16.5 and 3.5 Ma (Holes 335 and 332). Extension of this flow to 35 Ma (Hole 558) suggests either (1) a reversal of this trend between 35 and 18 Ma, if the most abundant LREE-enriched basalts from this hole are considered, or (2) no variation at all, if the only LREE-depleted basalt is taken at face value. Finally, near the approximate latitude of the 35°N anomaly flow line, the evidence suggests that the present-day anomaly persisted during the last 35 Ma and that local variations within a single hole or within the 35°N anomaly existed for at least the last 18 Ma. The variability in REE patterns increases from the fairly uniform in Hole 559, to the complex and rapidly fluctuating in Hole 561, and to the spike seen at 35°N on the present MAR axis (and superimposed on the general trend seen at the zero-age MAR axis).

Comparison of REE Data with Shipboard XRF Incompatible Trace Element Data

It is of geochemical interest and importance to compare the incompatibility trace element data obtained on board by XRF, used in constructing the extended Coryell-Masuda diagram (Coryell et al., 1963), and the REE results obtained by instrumental neutron activation analysis (INAA) from this study. Remembering that the XRF data and INAA are not obtained from exactly the same sample, La vs. Nb (Fig. 3A) shows a remarkable nearly one to one correlation for these two highly incompatible elements, despite the analytical problems that exist in measuring Nb at the low concentrations found in ocean basalts (Etoubeau et al., this vol.) The correlation exists for all samples, hence all holes, analyzed from Leg 82. Sm vs. Zr (Fig. 3B), representing two somewhat less incompatible elements, also shows a nearly one to one correlation. In summary the XRF and INAA results corroborate that the trace elements (specifically Nb, Zr, Ti, Y, and V) behave similarly to the rare-earths (e.g., La, Sm, Eu, Tb, and Lu) and can be used as analogs to compare other chemical parameters and mantle source domains. Their relative enrichment signatures (constructed with the trace element data) can be used as geochemical tracers for ocean areas, as is usually done with the rare-earth elements.

Downhole Variations

To examine the chemical groups and trends identified on board by XRF further, a comparison of the major el-

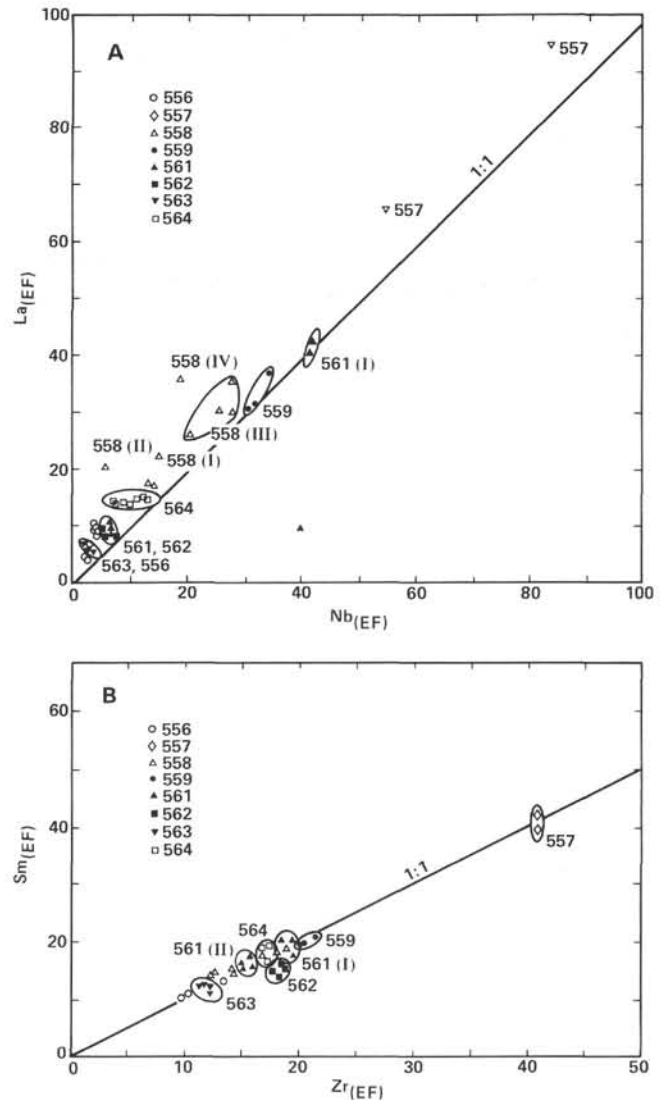


Figure 3. A. La versus Nb. All data are given in ppm. Roman numerals indicate chemical group (if more than one group was identified for the hole). Nd data are from site chapters, all sites except 560 (this volume), and La data, this report. Nb and La data are for sample horizons nearest to each other but not from identical samples. For further details of comparison see Rideout (1983). B. Sm versus Zr. All data are given in ppm. Zr data are from site chapters, all sites except 560 (this volume). Sm data are reported in Table 1.

ements from XRF and $(La/Sm)_{EF}$ from INAA is plotted versus depth in Figure 4. In general, Mg-number inversely correlates with Ti. In contrast, no systematic variation is observed between the $(La/Sm)_{EF}$ and Mg-number, suggesting a lack of a correlation between Mg-number and relative rare-earth patterns in these holes. The inverse correlation between incompatible element content and Mg-number has been interpreted as usually reflecting a lack of a chemical imprint caused by low-pressure crystallization (e.g., Bryan and Moore, 1977). Such an event would not affect and be recorded in the relative rare-earth enrichment patterns (Schilling, 1971). Either variable degrees of partial melting of a homogeneous mantle reservoir or variable mantle sources are necessary to explain the observed $(La/Sm)_{EF}$ variations.

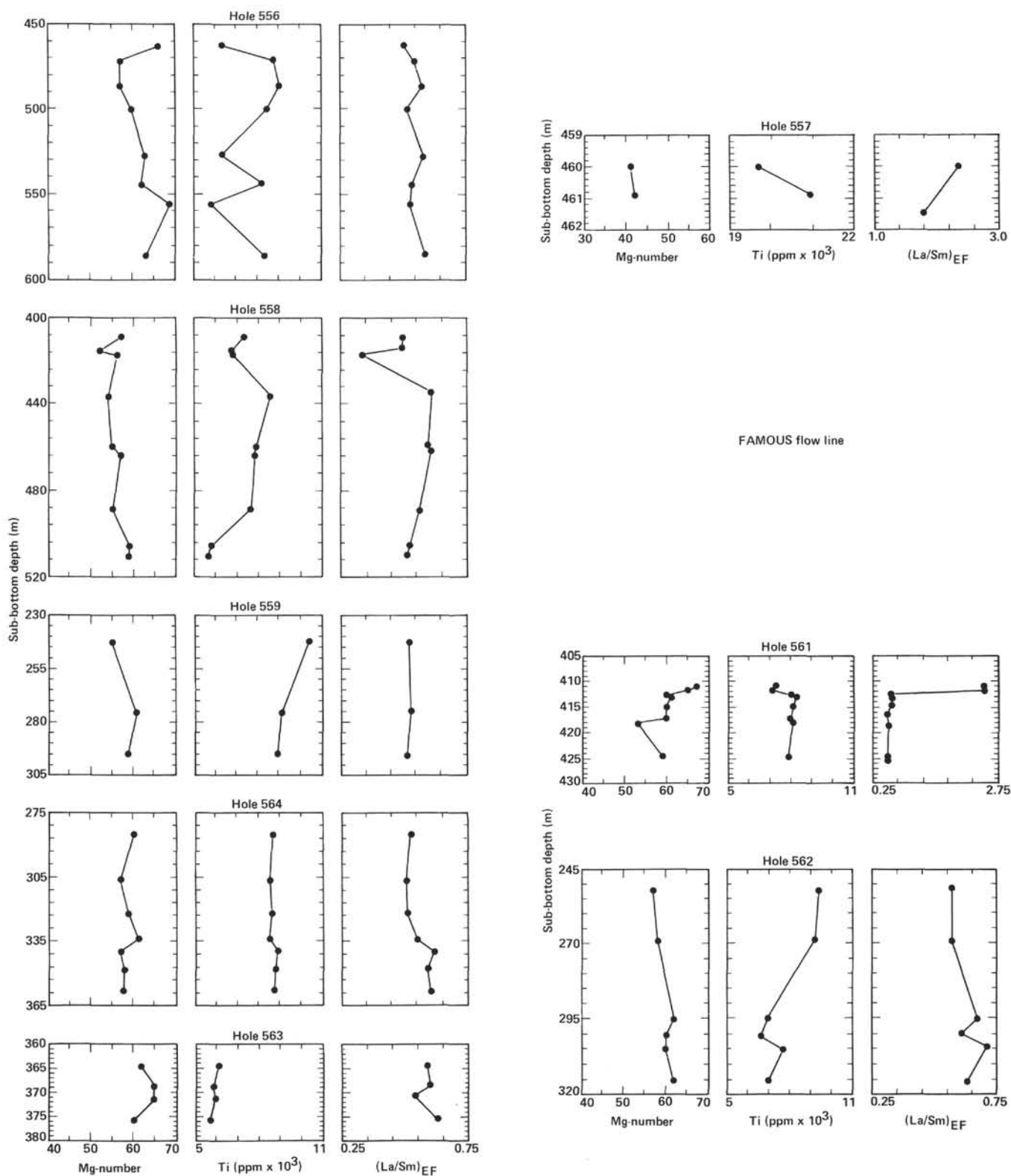


Figure 4. Mg-number, Ti, and (La/Sm)_{EF} versus depth along cores. Mg-number and Ti major element data are from the on-board X-ray fluorescence analyses, from site chapter, all sites except 560 (this volume). (La/Sm)_{EF} instrumental neutron activation data are from Table 1. For details of comparison, see Rideout (1983).

$^{143}\text{Nd}/^{144}\text{Nd}$ and $^{87}\text{Sr}/^{86}\text{Sr}$ Variations

The 15 samples selected for $^{143}\text{Nd}/^{144}\text{Nd}$ and $^{87}\text{Sr}/^{86}\text{Sr}$ isotope analyses represent at least 1 sample per hole for holes that have uniform REE patterns; 5 samples from Hole 558 and 2 samples from Hole 561 were analyzed in order to cover the range of depleted and light REE-enriched patterns present in these two holes. The $^{87}\text{Sr}/^{86}\text{Sr}$ and $^{143}\text{Nd}/^{144}\text{Nd}$ isotope ratio results obtained are listed in Table 2. Leaching experiments were conducted on a few selected samples (566-16-2, [Piece 15]; 558-38-1 [Piece 14]; 559-6-1 [Piece 5]; 561-1-1 [Piece 2C]) following the method of O'Nions and Pankhurst, (1976). These data are also shown in Table 2.

With one exception (558-28-2, Piece 16), $^{143}\text{Nd}/^{144}\text{Nd}$ versus $(\text{La}/\text{Sm})_{\text{EF}}$ (Fig. 5A) demonstrates that a good inverse correlation exists within and among holes, forming an inverse correlation between LREE fractionation patterns and $^{143}\text{Nd}/^{144}\text{Nd}$ isotope ratio signatures. An example illustrating the correlation within a single hole is shown in Figure 6A (Hole 561) and among holes by comparing Figures 6A and 6B (Holes 561 and 558). This correlation agrees well throughout the 18 and 35 Ma time periods, with the cited exceptions of Sites 558 and 561 (which will be discussed later).

In addition to the exception noted in Figure 5A, the $^{143}\text{Nd}/^{144}\text{Nd}$ versus $(\text{La}/\text{Sm})_{\text{EF}}$ correlation suggests that the spatial and temporal variations observed in the REE patterns must also be derived from mantle sources because the $^{143}\text{Nd}/^{144}\text{Nd}$ ratio is not likely to be affected by equilibrium partial melting or subsequent fractional crystallization involved in the generation and evolution of these basalts. Thus, the simplest explanation for the

Table 2. DSDP Leg 82: $^{87}\text{Sr}/^{86}\text{Sr}$ and $^{143}\text{Nd}/^{144}\text{Nd}$ isotope ratios.

Core-Section, Piece	Sub-bottom depth (m)	$^{87}\text{Sr}/^{86}\text{Sr}$ ± 2 SE	$^{87}\text{Sr}/^{86}\text{Sr}$ ± 2 SE (leached)	$^{143}\text{Nd}/^{144}\text{Nd}$ ± 2 SE	Sm/Nd
556-6-2, 2A	499.70	0.703156		0.513195	0.391
		28		22	
556-16-2, 15	586.36	0.703290	0.702855	0.513156	0.372
		26	28	18	
557-H1, CC	(1.74)	0.704141		0.512979	0.237
		30		20	
557-1-1, 10	461.45	0.703851		0.512952	0.284
		20		20	
558-27-3, 11B	409.17	0.703392		0.512999	0.317
		22		20	
558-28-1, 2	414.59	0.703251		0.512967	0.303
		22		20	
558-28-2, 16	417.31	0.703591		0.513025	0.423
		26		18	
558-33-1, 4	459.78	0.703378		0.512897	0.260
		24		20	
558-38-1, 14	505.59	0.703724	0.703210	0.512976	0.306
		34	44	22	
559-6-1, 5	274.93	0.703008	0.702985	0.513048	0.265
		30	26	16	
561-1-1, 2C	412.01	0.704028	0.703479	0.512940	0.284
		32	24	22	
561-2-3, 10A	418.62	0.703430		0.513102	0.401
		24		22	
562-7-1, 4B	295.32	0.703169		0.513139	0.448
		24		20	
563-24-3, 7F	370.75	0.703101		0.513137	0.404
		24		14	
564-5-2, 4B	322.53	0.702729		0.513127	0.374
		24		20	

Note: $^{87}\text{Sr}/^{86}\text{Sr}$ isotope ratio results are normalized to an E & A value of 0.70800 and $^{143}\text{Nd}/^{144}\text{Nd}$ isotope ratio results are normalized to a BCR-1 value of 0.512650. For error in Sm/Nd, see Schilling and Ridley, 1975. SE is standard error.

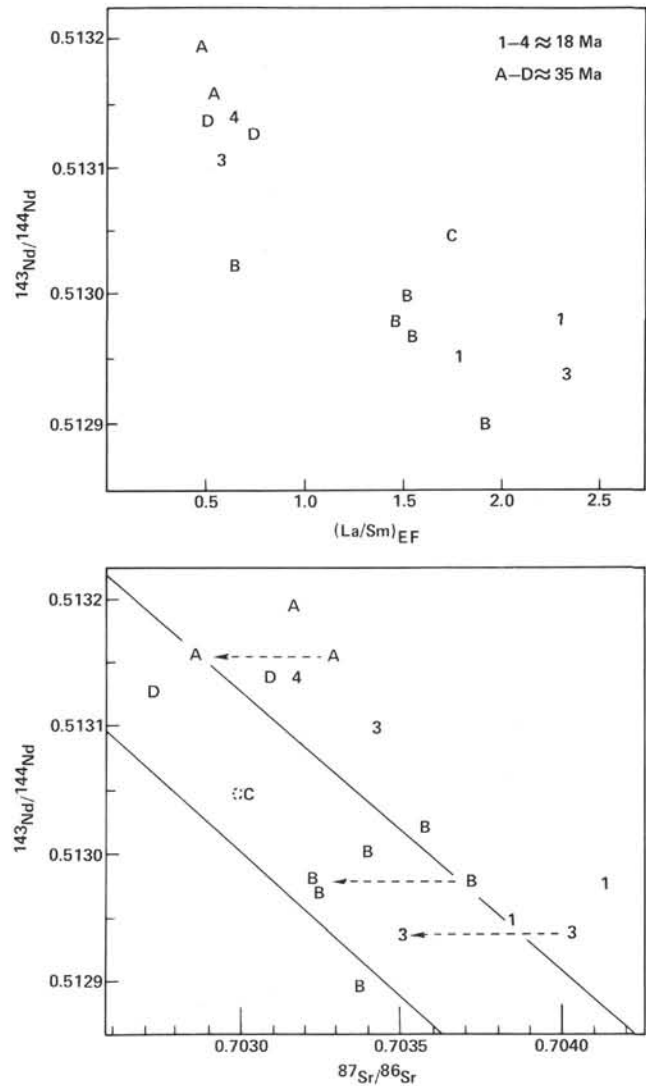


Figure 5. Top figure: $^{143}\text{Nd}/^{144}\text{Nd}$ versus $(\text{La}/\text{Sm})_{\text{EF}}$. Bottom figure: $^{143}\text{Nd}/^{144}\text{Nd}$ versus $^{87}\text{Sr}/^{86}\text{Sr}$. $^{87}\text{Sr}/^{86}\text{Sr}$ results from leached residues are indicated by dashed lines.

dispersion of the REE patterns and Nd isotopic ratios would be tapping of a heterogeneous mantle source.

It should be noted that the isotope ratios shown in Figure 5A and 5B are uncorrected for age. However, the age correction does not significantly affect the $^{143}\text{Nd}/^{144}\text{Nd}$ versus $(\text{La}/\text{Sm})_{\text{EF}}$ correlation, but only slightly alters the slope of the correlation line. The correction would range between 2 to 4×10^{-5} for the 18 Ma isochron and 4 to 6×10^{-5} for the 35 Ma isochron, for the LREE-enriched and LREE-depleted patterns, respectively.

Overall, the data presented in Figure 5 are broadly consistent with binary mixing, although it could be argued that the data cluster into two groups within this diagram, suggesting a lack of mixing. We suggest that these two clusters are an artifact of the sampling density, as the gap seen in the $(\text{La}/\text{Sm})_{\text{EF}}$ versus $^{143}\text{Nd}/^{144}\text{Nd}$ and $^{143}\text{Nd}/^{144}\text{Nd}$ versus $^{87}\text{Sr}/^{86}\text{Sr}$ space also corresponds to a gap in sampling between holes on the FAMOUS flow line and the 35°N flow line (Fig. 1). The distance

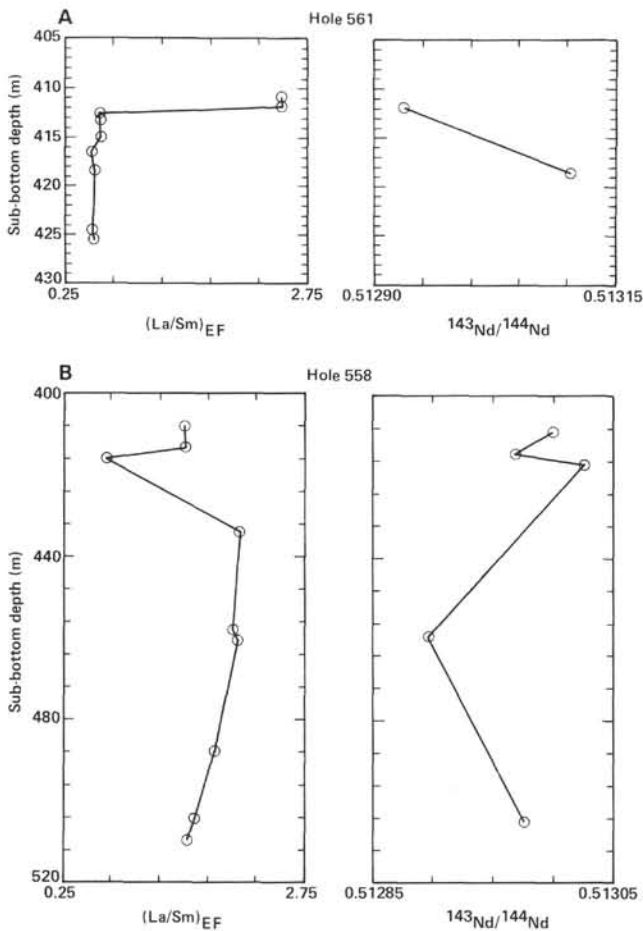


Figure 6. $(La/Sm)_{EF}$ and $^{143}Nd/^{144}Nd$ versus depth for Holes 558 and 561.

between these two flow lines is on the order of 390 km, as compared to ~100 km between the Azores and FAMOUS flow line and ~100 km between the flow line 35°N and the flow line south of the Hayes Fracture Zone. It is important to note that the samples analyzed in this study, therefore, are from widely separated sites and are irregularly spaced. The gap observed in Figure 5 could possibly be closed if the holes were closer together and the density of sampling was more homogeneous.

$^{143}Nd/^{144}Nd$ versus $^{87}Sr/^{86}Sr$ (Fig. 5B) also shows an inverse correlation, but with significantly greater scatter. In general, the data fall within the so-called mantle array (using boundary lines that are two sigma deviations from a linear best fit to average ocean basalt values (Waggoner, in prep.)³. The scatter is predominantly to the right of the array and seems to have been caused by seawater alteration, which enhances the $^{87}Sr/^{86}Sr$ ratios of the basalts, whereas the $^{143}Nd/^{144}Nd$ ratios remain essentially unaffected (O’Nions and Pankhurst, 1976). Leaching experiments were conducted on samples suspected of having various degrees of $^{87}Sr/^{86}Sr$ enhancement from seawater alteration (including a sample that appeared not to have been so affected) to check the

leaching technique and assumptions. Results of these experiments are presented in Table 2 and are indicated by the dashed lines in Figure 5. Samples displaced to the left are observed to plot closer or on the trend of the mantle array upon leaching, whereas one sample (symbol C) that plotted on the mantle array trend was not affected by the leaching, thus confirming seawater alteration. However, this presents an uncertainty in the $^{87}Sr/^{86}Sr$ data, so care must be taken to use the corrected $^{87}Sr/^{86}Sr$ data, within or contiguous to the mantle array for later comparison.

In order to compare the rare-earth and isotope ratio effects in time and space, $(La/Sm)_{EF}$, $^{143}Nd/^{144}Nd$, and $^{87}Sr/^{86}Sr$ are shown plotted against latitude in Figure 7. The dashed envelopes shown in the $(La/Sm)_{EF}$ and $^{87}Sr/^{86}Sr$ are the data for the zero-age Mid-Atlantic Ridge

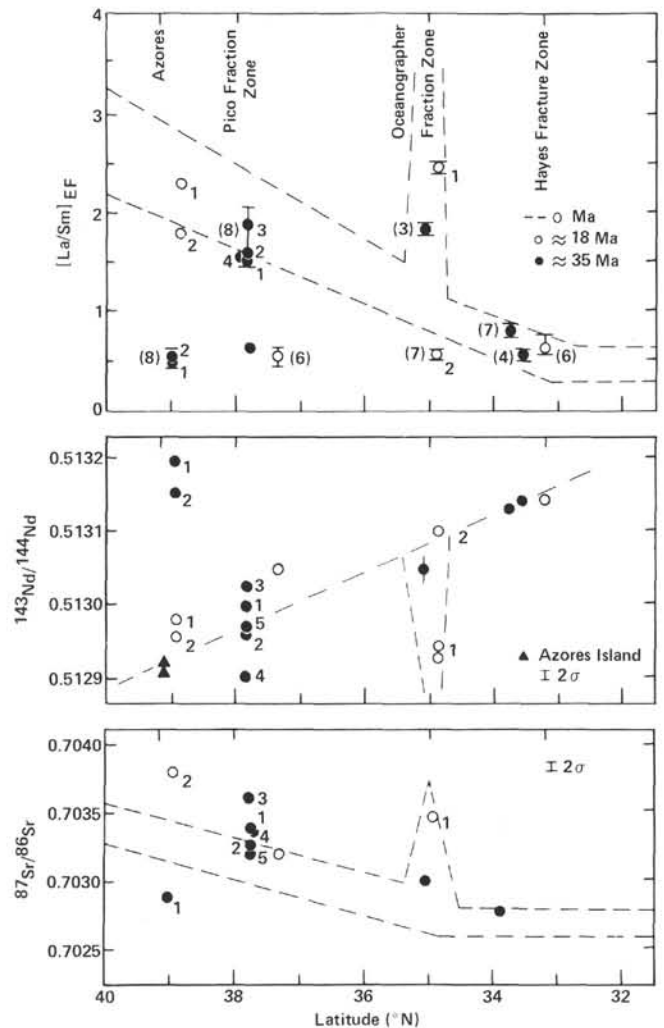


Figure 7. $(La/Sm)_{EF}$, $^{143}Nd/^{144}Nd$, and $^{87}Sr/^{86}Sr$ results plotted versus latitude. Dashed lines for the zero-age variation are taken for REE from Schilling (1975) and for $^{87}Sr/^{86}Sr$ from White and Schilling (1978); $^{143}Nd/^{144}Nd$ line is inferred from $^{87}Sr/^{86}Sr$ data and the mantle array relationship for ocean basalts. Open circles are for 18 Ma and closed circles are for 35 Ma isochrons. $^{87}Sr/^{86}Sr$ data plotted are results that fall within or adjacent to the $^{143}Nd/^{144}Nd$ versus $^{87}Sr/^{86}Sr$ mantle array (Fig. 6B) and the leached samples.

³ Waggoner, D. G. [Ph.D. dissert.] University of Rhode Island, Kingston.

(Schilling et al., 1983; White and Schilling, 1978). The dashed line on the $^{143}\text{Nd}/^{144}\text{Nd}$ diagram is an estimate of where the zero-age data would be, based on what data are now available and the correlation of $^{143}\text{Nd}/^{144}\text{Nd}$ to $^{87}\text{Sr}/^{86}\text{Sr}$ generally observed in mid-ocean ridge basalts and Figure 5.

The data are observed to generally follow the present day Mid-Atlantic Ridge trends (as indicated by the dashed lines) with the exceptions previously noted, namely Holes 556 (35 Ma, Azores Platform flow line) and 335 (16 Ma, FAMOUS flow line), both of which are uniformly LREE depleted, and a single horizon in Hole 558, which is also depleted in LREE but has a low $^{143}\text{Nd}/^{144}\text{Nd}$ ratio comparable to the basalts with LREE-enriched patterns that dominate this hole.

Thus, it would seem that a tendency for the development of a chemical gradient already existed in the past, with the exceptions noted above and below. In particular, the Nd isotope data in Figure 7 suggest that:

1. Anomalous Azores mantle enrichments were never present south of the Hayes Fracture Zone, thus, providing further evidence that the source of the depleted MORBs that occur worldwide is to a first order uniform or well mixed.

2. The enriched Azores mantle anomaly apparently was not present 35 Ma ago, as seen in the depleted LREE signature of Hole 556, and must have appeared between 35 and 18 Ma to generate the enriched LREE patterns seen at Hole 557.

3. The gradient resulting from the enriched Azores mantle anomaly, 16.5 Ma ago, if at all present, did not extend down to the latitude of the FAMOUS flow line, as seen in the depleted LREE signature of Hole 335, Leg 37; rather, it began some time after, as seen by the increasing degree of LREE enrichment from Hole 332 (approximately 16 Ma) to the zero-age MAR axis.

4. The 35°N mantle anomaly has persisted for the last 35 Ma and influenced the eruptive products at the Mid-Atlantic Ridge axis at this latitude and time period and, thus, the corresponding flow lines as well. The large local variations (irregular mixing?) along this flow line seem to have appeared only 18 Ma ago.

5. Points 1-4 illustrate the presence of long-term, large-scale source variations in this region, whereas Hole 561 reflects short-term source variations.

6. A special explanation is necessary for Hole 558, which is anomalous in two ways: (1) we have noted that the inverse correlation between $^{143}\text{Nd}/^{144}\text{Nd}$ versus $(\text{La}/\text{Sm})_{\text{EF}}$ breaks down for the only lava horizon from this hole that has a LREE-depleted pattern (i.e., 5587-28-2 [Piece 16]); and (2) the LREE-enriched patterns with low $^{143}\text{Nd}/^{144}\text{Nd}$ from Hole 558 cannot be related to the Azores hot spot anomaly, because the Azores anomaly does not appear to be present at 35 Ma along the Azores flow line.

We will now briefly discuss the anomaly in this hole.

Sample 558-28-2 (Piece 16) is the only sample found in Hole 558 with a horizon characterized by a depleted LREE pattern (Fig. 2). It has a low $^{143}\text{Nd}/^{144}\text{Nd}$ for such a depleted pattern, falling in the upper part of the range of basalts with enriched LREE patterns from the same hole and other holes from Leg 82.

The discrepancy may suggest LREE depletion must be relatively recent, so that radiogenic ^{143}Nd had not had time to accumulate (Fig. 5B). Figures 4 and 5B show that this horizon is also systematically lower in Mg-number, Ti, and $(\text{La}/\text{Sm})_{\text{EF}}$ relative to the chemical horizons above it or below it. Fractional melting with some garnet in the residue (Wood, 1979; 1981; Zindler et al., 1979) or dynamic melting (Langmuir et al., 1977) could be suggested to explain the presence of this anomalous chemical horizon and the crossing of the rare-earth patterns in the HREE within this hole. Such short-term fluctuations between sources within a single hole implies the absence of a well-mixed magma chamber or a wide zone of melting where interstitial melt droplets coalesce and mix. A rapid transfer of magma from the time of melting to the time of eruption is also implied.

Finally, $^{143}\text{Nd}/^{144}\text{Nd}$ versus Sm/Nd (Fig. 8) further demonstrates that the depleted sample also has an anomalously high $^{143}\text{Nd}/^{144}\text{Nd}$ for its Sm/Nd value plotted relative to the other LREE-enriched samples from this hole. An isochron line drawn through the four enriched samples yields a slope with an age of approximately 437 Ma (Fig. 8A). This can be further evaluated by Figures 8B and 8C, which include the data from Holes 558 and 561, and all the holes, respectively. Indeed, with the exception of the depleted sample from Hole 558 (558-28-2 [Piece 16]), the samples fall along broad linear correlation trends, corresponding respectively to ages of 362 Ma (Fig. 8B) and 310 Ma (Fig. 8C) if interpreted as isochrons (Table 3). Interestingly enough, the estimated ages fall in the range dating the earliest time (model age) that the enriched Azores source and the depleted MORB source could have been produced from a common source, based on the $^{87}\text{Sr}/^{86}\text{Sr}$ and Rb/Sr ratios of dredged basalts along the present MAR axis (White and Schilling, 1978). However, it is also possible that the line represents variable mixing between an enriched mantle component and depleted asthenospheric material. These two alternative models can be combined by assuming that the mixing event responsible for the large spectrum of variations observed between these two extreme mantle domains occurred subsequently.

INTERPRETATION AND DISCUSSION

In the previous discussion, fractional crystallization and partial melting have been eliminated as the primary causes of the temporal and spatial variations in REE patterns and $^{143}\text{Nd}/^{144}\text{Nd}$ isotopic variations seen in the Leg 82 study area. Dynamic melting may explain the complex geochemical patterns observed at Hole 558. Otherwise, the geochemical variations must reflect mantle heterogeneities and their possible dynamic interaction. Interpretation of the results in terms of mantle dynamics may be accomplished by considering two extreme models:

1. A veined or lumpy mantle that contains a random distribution of enriched domains of variable size and shape, all passively embedded in a LILE-depleted convecting upper mantle (e.g., Davies, 1981; Richter and Ribe, 1979); or

2. A mantle dominated by the interaction and mixing of buoyant, independently rising, LILE-enriched blobs

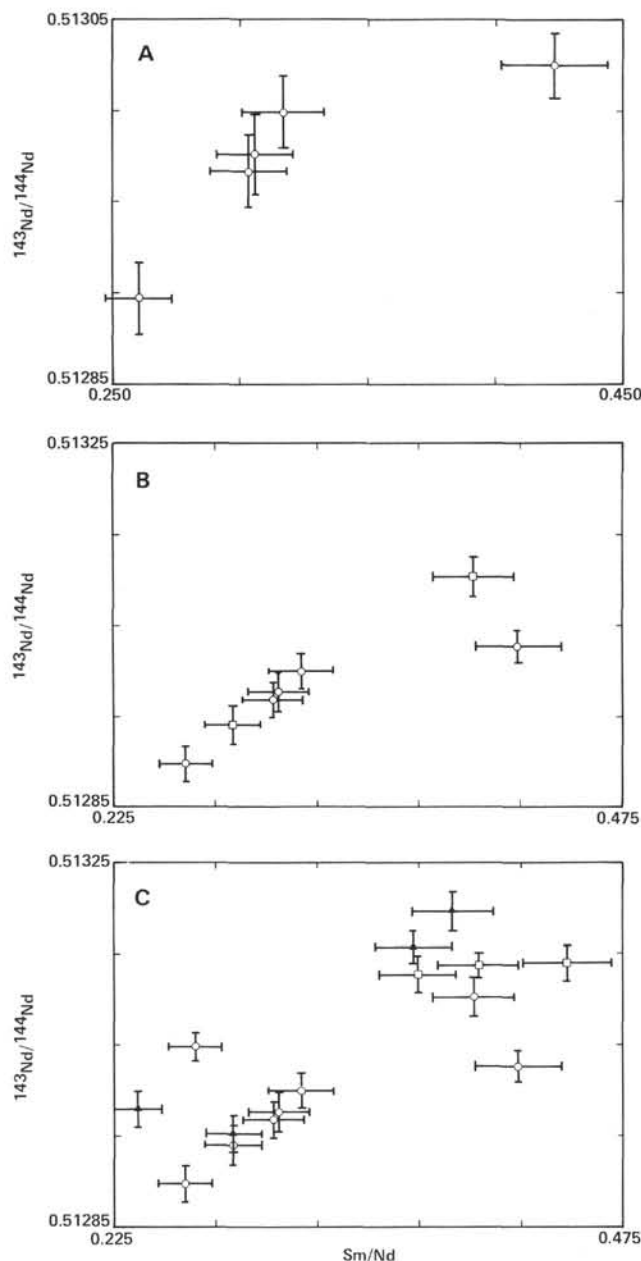


Figure 8. $^{143}\text{Nd}/^{144}\text{Nd}$ versus Sm/Nd using data population from A. Hole 558 only. B. Holes 558 and 561 combined (circles are for 558, squares for 561). C. The eight holes studied from Leg 82 (circles for Holes 558, 559, and 561, along the FAMOUS and 35°N flow lines; triangles for Holes 556 and 557, along the Azores flow line; squares for Holes 562, 563, and 564, south of the Hayes Fracture Zone).

(plume) with LILE-depleted asthenospheric material—a model formulated within the framework of fixed hot spots (or mantle plume) and migrating spreading ridges (Morgan 1971; 1981).

Model One: Random Distribution of Enriched Material within the Mantle

The first model could explain many of the geochemical observations for this region. Long-term and large-scale variations, seen along flow lines and along the

Table 3. $^{143}\text{Nd}/^{144}\text{Nd}$ versus Sm/Nd age calculations.

Coefficient or variable	Figure 8A	Figure 8B	Figure 8C
y_0	0.512446	0.512534	0.512639
m	2.86×10^{-3}	2.37×10^{-3}	2.03×10^{-3}
C	0.998	0.995	0.846
t	437×10^6	362×10^6	310×10^6

Note: Calculations use the radiogenic equation, $^{143}\text{Nd}/^{144}\text{Nd} = (^{143}\text{Nd}/^{144}\text{Nd})_0 + (^{147}\text{Sm}/^{144}\text{Nd})(e^{\lambda t} - 1)$ and solving in the form, $y = mx + b$.

$^{147}\text{Sm}/^{144}\text{Nd}$ values approximated from instrumental neutron activation analysis data by $^{147}\text{Sm}/^{144}\text{Nd} - \text{Sm}/\text{Nd} \times 0.6049$.

The slope, m , is obtained from regression of the data given in Tables 1 and 2 and summarized in Table 2. Correlation coefficients, C , are solved for dependent variables. Ages are obtained by substituting slope (m) and decay constant $\lambda = 6.54 \times 10^{-12}$ into $t = (1/\lambda) \ln(m + 1)$.

ridge axis, could be a result of sampling of larger enriched bodies. Within these small bodies, small scale variations could be attributable to smaller bodies (with their own geochemical signature) lying within the domain of the larger bodies. Short-term and small-scale variations could be the result of (many) smaller bodies or many such bodies overlapping and mixing with each other and the depleted asthenospheric material in which they are embedded. Corrective stirring of the original anomaly of whatever size would result in a random and variable distribution of the original anomaly, depleted asthenosphere, and the products of mixing between the anomalies and the depleted asthenosphere (Richter and Ribe, 1979).

Thus, the first model can explain just about anything observed in the Leg 82 results, because the model is essentially unconstrained, but it can not explain everything well. This random model would require a special explanation to account for the zero-age observations (i.e., the regular gradient observed along the Mid-Atlantic Ridge axis as previously noted). We are unaware of any such explanation.

Model Two: Mantle Plume—Migrating Ridge Interactions

Morgan (1978) and Schilling and co-workers (1983) have shown that the mode of interaction of the LILE-enriched plume and the LILE-depleted asthenospheric material is a function of the relative distance from the ridge to the hot spot. The hot spot is defined as a source of the material, and the migrating spreading ridge acts as a sink for the material (see Vogt, 1976).

Three phases of such hot spot-lithosphere interactions can conveniently be described for the sake of discussion, namely, (1) a ridge-centered hot spot, (2) a near-ridge hot spot, once over the ridge but the ridge has since migrated, and (3) a purely intraplate hot spot.

In the central North Atlantic, Schilling (1973; 1975) and Schilling et al. (1983) have shown that the gradient south of Iceland and the Azores are a result of ridge-centered hot spot-spreading ridge interaction. In this case Schilling and Noe-Nygaard (1974) have suggested that when the flux of plume material is in excess of what is

needed by the above spreading ridge, the excess is assimilated in two ways, (1) by building up a thicker crust (e.g., Iceland), and (2) by laterally flowing along the ridge axis, where the enriched plume material is progressively mixed with LILE-depleted asthenospheric material until there is no more left and a large-scale chemical gradient is observed in Layer 2A. The same process is envisioned south of the Azores Platform where a chemical and topographic gradient is observed down along the MAR axis up to the Hayes Fracture Zone (Schilling, 1975; White and Schilling 1978; Bougault and Treuil, 1980). In this case, local uniformity is observed along the gradient, such as in the FAMOUS region (White and Bryan, 1977; White, 1979; Dupre et al., 1981).

As the ridge moves away from the hot spot and the distance between the hot spot and ridge increases, a channel is established between the ridge (sink) and the hot spot (source), e.g., the Galapagos (Morgan, 1978; Schilling et al., 1983; Verma et al., 1983). The chemical gradient seen at the spreading ridge contracts finally to a point source, characterized as a spike of enriched anomalous material as the sub-ridge axial flow decreases and finally stops. Schilling et al. (1983, 1985) have also suggested that the sublithospheric flow from the hot spot to the ridge decreases also as the distance to the ridge increases, resulting in poor mixing and large variability in the geochemistry within that single anomalous data spike. Finally, the distance increases so much that the channel cannot connect to the ridge any longer and the hot spot becomes intraplate (e.g., Hawaii). There is no

further direct interaction between the hot spot and the material normally feeding the spreading ridge.

Thus, the degree of variability observed in the product of mixing between the enriched and depleted material increases as the hot spot moves farther away from the ridge itself.

Two types of hot spots have been identified from kinematic studies in the central North Atlantic: (1) the Azores hot spot, which is believed to have become ridge centered only recently (i.e., when migrating Mid-Atlantic Ridge approached the hot spot and became ridge centered, approximately 20 Ma [Morgan 1981]), and (2) the so-called New England hot spot, which was intraplate beneath the North American plate from ~140 Ma to > ~80 Ma, intersected the ridge ~80 to 60 Ma ago, and since then has been overlain by the African plate (Morgan, 1981; Duncan, 1983; see Figure 9).

Within this model, the results from Legs 82 and 37 can be interpreted in the following way: (1) Holes 556 and 557 (Leg 82); Holes 335, 332A, and 332B (Leg 37); and the FAMOUS region provide evidence for the appearance of the Azores plume (blob) between 35 and 18 Ma and the progressive positioning of the Mid-Atlantic Ridge over it; and in contrast, (2) Holes 559 and 561 (Leg 82) along the approximate 35°N flow line reflect the migration of the Mid-Atlantic Ridge axis away from the New England hot spot over the past 35 Ma. The connection between the hot spot and the ridge need not have followed the most direct (shortest) and simplest route possible as the ridge migrated. Hole 558 is the on-

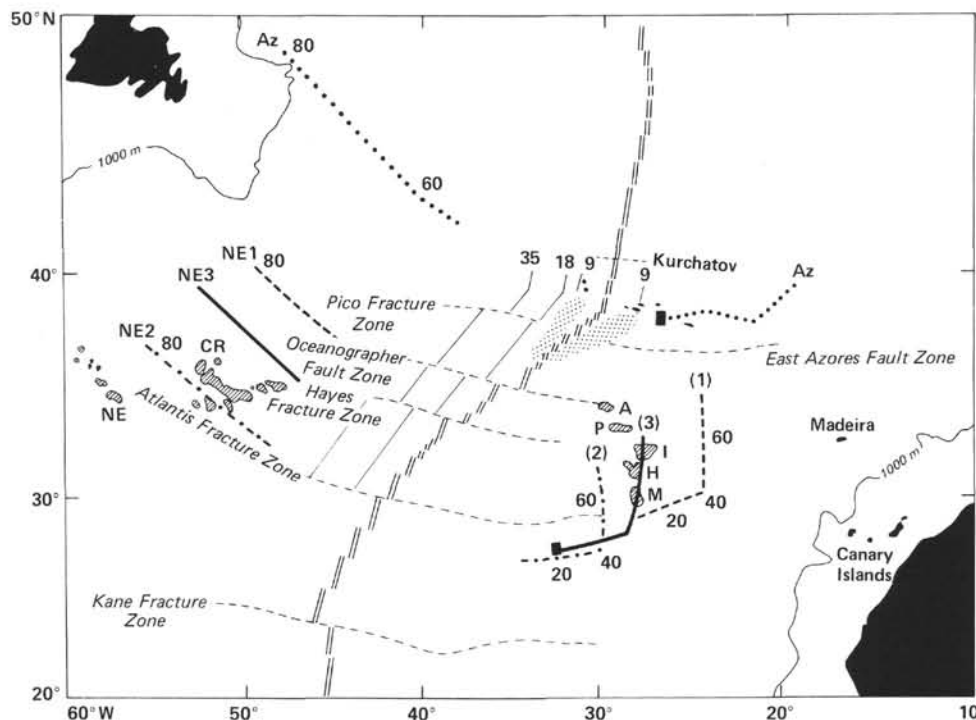


Figure 9. Tracks of the Azores (Az) and New England hot spots based on the following reconstructions: NE1 from Morgan (1981), Azores and NE2 from Duncan (1982), and NE3 from Duncan (1983). Stippled areas represent V-shaped time-transgressive ridges based on 1000-m contour lines, compiled from Olivet (1982), Vogt and Tucholke (1979), and Saemundsson (1984). Map modified from Cande et al. (1983). Symbols for seamounts are A: Atlantis, P: Platon, I: Irving-Cruiser, H: Hyer, M: Great Meteor, NE: New England, and CR: Corner Rise.

ly hole that is not explained by either of these models and requires additional discussion.

We now elaborate further on these two interpretations within the context of this model.

Azores hot spot. South of the Hayes Fracture Zone, all the material at Holes 562, 563, and 564, representing 18 and 35 Ma respectively (Fig. 1), is depleted. This agrees with the depleted signature for material seen at the present day Mid-Atlantic Ridge, suggesting that the Azores mantle anomaly never extended beyond the Hayes Fracture Zone during the last 35 Ma. It may be possible that the Hayes Fracture Zone is a physical barrier to flow of material from the Azores hot spot southward along the MAR; however, if this is so, it has assumed this function only recently.

Along the flow line at the latitude of the Azores anomaly, Hole 556 (approximately 35 Ma) is depleted. Thus, at 35 Ma, there is no evidence of a hot spot mantle plume (blob) at the latitude of the Azores. However, Hole 557 (approximately 18 Ma) is enriched. Hole 557 is interpreted as related to the ridge-centered Azores hot spot, known to be producing enriched material at the zero-age Mid-Atlantic Ridge. Therefore, one can postulate that the Azores hot spot blob rose through the lithosphere and began and/or manifested itself at some time between 35 and 18 Ma (i.e., between the time range sampled at Holes 556 and 557). Note, however, that only 1.5 m of actual core was retrieved from Hole 557.

Variation along the flow line of the FAMOUS region, (Holes 335, 332A, and 332B, Leg 37, and FAMOUS) suggest that subridge axial flow from the Azores plume had not reached the latitude of the FAMOUS flow line at 16 Ma (if Hole 559 is excluded). Subsequent mixing of the enriched Azores mantle plume with the depleted asthenosphere resulted in mixing products progressively enriched from 16.5 Ma to present. This interpretation is independently supported by the time transgressive V-shaped ridge branching from Flores and Pico (approximately 9 Ma) and meeting the MAR axis around 36°N, as shown in Figure 9. This is also shown in the topographic map of Olivet et al. (1982) and is discussed by Vogt et al. (unpublished paper⁴) and by Saemundsson (in press). Furthermore, Morgan (1981), in a kinematic reconstruction of plate motions relative to the fixed hot spot reference frame in the Atlantic, suggests that the Azores hot spot appears at the Earth's surface on the Eurasian plate only 20 Ma ago and since has been progressively approached by the Mid-Atlantic Ridge axis, which in this fixed reference frame has been migrating southwestward, leaving its trail on the Eurasian plate only (Fig. 9). This other independent evidence is broadly consistent with the isotope data, because the kinematics suggest that the Azores hot spot would become ridge centered only later than 20 Ma, as the plume-like isotope signature is apparent on the ridge axis for the first time only 18 Ma ago (Hole 557). However, our interpretation would be inconsistent with Duncan's reconstruction, which assumes that the Azores hot spot was con-

tinuously active for the last 80 Ma as reflected by the Newfoundland-Labrador Ridge (Fig. 9). Therefore, the LILE-depleted source present 35 Ma ago (Hole 556) would not be explained.

New England hot spot. A deviation from the uniform transitional REE patterns seen at the zero-age MAR axis is observed at ~35°N, expressed as a spike of LREE-enriched material above the uniform, slightly light REE-enriched patterns of the transitional ridge. The 35°N geochemical anomaly, represented by the enriched plume-like material, is superimposed over the large-scale gradient along the present-day MAR axis and is also observed on the 35 and 18 Ma isochrons, Holes 559 and 561, respectively. Thus, the anomaly seems to have persisted over the last 35 Ma. Large variability of source derivation is seen within this spike only since 18 Ma (Hole 561 and the present ridge axis). Only typically enriched or depleted mantle sources are observed in Hole 561, but intermediate types are also observed in the present day 35°N anomaly. We have indicated that this seems to be representative and characteristic of near-ridge hot spots (e.g., Schilling et al., 1983). Thus, these geochemical anomalies are interpreted as being related to a near-ridge hot spot. The question remaining is—which hot spot?

Kinematic reconstructions of plate motion relative to the reference frame of fixed hot spots have been studied in the North Atlantic by Morgan (1981), Duncan (1981, 1982, 1983), Olivet et al. (1982), and Burke et al. (1973). Reproduction of the trace left by the New England and Azores hot spots is shown in Figure 9, for the reconstructions of Morgan (1981) and Duncan (1982, 1983) and modified from the work of Cande (this vol.). It appears that the New England hot spot, represented by the New England Seamounts on the west flank of the MAR and the Great Meteor-Atlantis Seamount trail on the east side of the MAR, brackets the 35°N anomaly revealed along the 35°N flow line. Thus, within the uncertainty of plate reconstructions, the 35°N anomaly trace over the past 35 Ma could be the result of the activity of the New England hot spot. The present location of this hot spot is also uncertain. Burke et al. (1973), calling this the Colorado hot spot, placed it just north of the Oceanographer Fracture Zone at 34°N, 37.5°W. Morgan (1981) gave the present hot spot coordinates within his model as 22°N, 29°W, (or 29°N, 30°W for a more recent construction involving the Cruiser-Great Meteor Seamounts as a track on the African plate). Duncan (1982), using age determinations and correcting for the relative and absolute motion of North America and Africa, gave the present position of the New England Seamount hot spot at 27°N, 35°W. We conclude that, within these uncertainties, it is reasonable to assume that the 35°N hot spot regime reflects the New England plume activity and flow towards the migrating MAR over the last 35 Ma.

Hole 558. Hole 558 (approximately 35 Ma), on the latitude of the FAMOUS flow line, is not only the most complex of all the holes sampled but is the most difficult to explain by any model. Hole 558 is predominantly LREE enriched, with the exception of 558-28-2 (Piece 16), a LREE-depleted sample discussed earlier (which

⁴ Vogt, P. R., Egluff, J., Johnson, G. L., and Perry, R. K., 1979. The Faial-Flores time-transgressive ridges: evidence for southward asthenospheric flow from the Azores mantle plume?

probably is related to recent fractional melting). Within the framework of the plume model, the enriched material seen in this hole cannot be simply explained by subridge axial flow from the Azores plume, because the evidence presented here indicates that the plume had not reached the surface 35 Ma ago. The hole is also quite far from the New England plume, which suggests a northward subridge axial flow from this plume 35 Ma ago. In any case, plate reconstructions indicate that the migrating MAR axis was centered over this hot spot in the period of 80–60 Ma, not 35 Ma.

We conclude that the enriched nature of the source of basalts from Hole 558 remains unexplained within the framework of the plume-migrating MAR axis model, whether the New England or the Azores hot spot plumes are considered. However, it must also be realized that the Corner Seamounts do not fit the New England hot spot trace as proposed in the reconstructions of Morgan (1981) or Duncan (1983). Could it be that the Hole 558 enriched mantle source anomaly is related to the activity of the Corner Seamounts (McGregor and Krause, 1972)? Clearly, to test this possibility we would need better sampling as well as more accurate plate reconstructions.

CONCLUSIONS

The isotopic and REE data in basalts obtained from the eight holes drilled during Leg 82 reflect large-scale, long-term as well as smaller scale, short-term time variations of mantle sources present beneath the MAR over the last 35 Ma of its spreading activity. These variations can be fully explained by a mantle model in which the mantle is veined or lumpy and contains a random distribution of enriched domains of variable size and shape, all passively embedded in the LILE-depleted convecting upper mantle, as proposed by Davies (1981) and Richter and Ribe (1979).

With one notable exception (Hole 558), the variations can also be explained within the more restrictive model that hypothesizes interaction and mixing of buoyant, independently rising, LILE-enriched blobs (plumes) with LILE-depleted asthenospheric material—a model formulated within the framework of fixed hot spots (plumes) and a migrating, spreading MAR axis. The variations observed within this model framework require that at least two hot spots—the Azores and the New England hot spots—be considered. The variation along the 35°N flow line (Holes 559 and 561) reflect the flow and mixing over the last 35 Ma of the New England plume toward the migrating MAR axis and poor mixing conditions over the last 18 Ma. On the other hand, variations within Holes 556 and 557 and from Leg 37 suggest that the Azores plume did not leave its imprint along the migrating MAR before 18 Ma ago, and flow along the ridge occurred only later. These inferences are consistent with (1) plate reconstructions within the framework of fixed hot spots, which suggest that the Azores plume appeared on the Earth's surface only 20 Ma ago and which provide a trace of the New England hot spot whose uncertainties bracket the anomalous 35°N flow line, and (2) the V-shaped time-transgressive ridge converging southward towards the MAR from Flores and Pico, which

suggests that a subaxial flow downridge started around 9 Ma ago.

It is conceivable, but not proven, that the enriched source of basalt for Hole 558, which cannot readily be explained by either of the two plume models, may be related to the activity of the Corner Seamounts (McGregor and Krause, 1972), which could (possibly) represent a third plume.

Finally, the short-term fluctuation observed between sources in Hole 561 implies rapid transfer of magma from the time of melting until eruption and provides evidence contrary to (1) the presence of a well-mixed magma chamber or (2) a wide zone of melting where magma droplets coalesce and mix at this particular location and time. Intense fracturing extending to the zone where melts are found could conceivably explain this particular situation.

ACKNOWLEDGMENTS

We thank F. DiMeglio and his staff for neutron activations and facilities at the Rhode Island Nuclear Science Center. This work was partly supported by NSF under Grants OCE 8200137 and OCE 8208014.

REFERENCES

- Aumento, F., Melson, W. G., et al., 1977. *Init. Repts. DSDP, 37*: Washington (U.S. Govt. Printing Office).
- Bougault, H., and Treuil, M., 1980. Mid-Atlantic Ridge: zero-age geochemical variations between the Azores and 22°N. *Nature*, 286:209–212.
- Bryan, W. B., and Moore, J. G., 1977. Compositional variation of young basalts in the Mid-Atlantic Ridge rift valley near 36–46°N. *Geol. Soc. Am. Bull.*, 88:556–570.
- Burke, K., Kidd, W. S. F., and Wilson, J. T., 1973. Relative and latitudinal motion of Atlantic hot spots. *Nature*, 245:133–137.
- Cande, S. C., Bougault, H., Hill, L., Morgan, W. J., and Schouten, H., 1983. North Atlantic hot spot tracks and the pattern of enriched or depleted basalts in Leg 82 drill holes. *EOS, Trans. Am. Geophys. Union*, 64(18):345. (Abstract)
- Coryell, C. D., Chase, J. W., and Winchester, J. W., 1963. A procedure for geochemical interpretation of terrestrial rare-earth abundance patterns. *J. Geophys. Res.*, 68:559–566.
- Davies, G. F., 1981. Earth's neodymium budget and structure and evolution of the mantle. *Nature*, 290:208–213.
- Duncan, R. A., 1981. Hotspots in the southern oceans—an absolute frame of reference for the motion for of Gondwana continents. *Tectonophysics*, 74:29–42.
- , 1982. The New England Seamounts and the absolute motion of North America since mid-Cretaceous time. *EOS, Trans. Am. Geophys. Union*, 63:1103–1104.
- , 1983. The position of the North Atlantic spreading ridges in the hotspot reference frame, Cretaceous to Present. *EOS, Trans. Am. Geophys. Union*, 64:345.
- Dupre, B., Lambret, B., Rousseau, D., and Allegre, C. J., 1981. Limitations on the scale of mantle heterogeneities under oceanic ridges. *Nature*, 294:552–554.
- Hart, S. R., and Brooks, C., 1974. Clinopyroxene matrix partitioning of K, Rb, Cs, Sr, and Ba. *Geochim. Cosmochim. Acta*, 38: 1799–1803.
- Langmuir, C. H., Bender, J. F., Bence, A. E., Hanson, G. N., and Taylor, S. R., 1977. Petrogenesis of basalts from the FAMOUS area: Mid-Atlantic Ridge. *Earth Planet. Sci. Lett.*, 36:133–156.
- McGregor, B. A., and Krause, D. C., 1972. Evolution of the seafloor in the Corner Seamounts area. *J. Geophys. Res.*, 77:2525–2534.
- Morgan, W. J., 1971. Convection plumes in the lower mantle. *Nature*, 230:42–43.
- , 1978. Rodriguez, Darwin, Amsterdam, . . . , A second type of hotspot island. *J. Geophys. Res.*, 83:5355–5360.

- _____, 1981. Hotspot tracks and the opening of the Atlantic and Indian Oceans. In Emiliani, C. (Ed.), *The Sea* (Vol. 7): New York (J. Wiley and Sons), 443-487.
- Olivet, J. L., Bonnin, J., Beuzart, P., and Auzende, J. M., 1982. Cinématique des plaques et paléogéographie: une revue. *Bull. Soc. Geol. Fr.*, 7:?
- O'Nions, R. K., Hamilton, P. J., and Evensen, N. M., 1977. Variations in $^{143}\text{Nd}/^{144}\text{Nd}$ and $^{87}\text{Sr}/^{86}\text{Sr}$ ratios in oceanic basalts. *Earth Planet. Sci. Lett.*, 34:13-22.
- O'Nions, R. K., and Pankhurst, R. J., 1976. Sr-isotopes and rare-earth element geochemistry of Deep Sea Drilling Project Leg 37 basalts. *Earth Planet. Sci. Lett.*, 31:255-261.
- Richter, F. M., and Ribe, N. M., 1979. On the importance of advection in determining the local isotopic composition of the mantle. *Earth Planet. Sci. Lett.*, 43:212-222.
- Rideout, M. L., 1983. DSDP Leg 82: spatial and temporal variations in the central North Atlantic [M. S. Thesis]. University of Rhode Island, Kingston.
- Saemundsson, K., in press. Subaerial volcanism in the western North Atlantic. *The Decade of North American Geology (DNAG) Synthesis*, (Vol. 1: The Western Atlantic Region): Washington (Geol. Soc. Am.), DNAG Special Publications.
- Schilling, J.-G., 1971. Sea-floor evolution: rare-earth evidence. *Phil. Trans. R. Soc. London., Ser. A*, 268:663-706.
- _____, 1973. Icelandic mantle plume: geochemical study of Reykjanes Ridge. *Nature*, 242:265-273.
- _____, 1975. Azores mantle blob: rare-earth evidence. *Earth Planet. Sci. Lett.*, 25:103-115.
- Schilling, J.-G., Kingsley, R., and Bergeron, M., 1977. Rare earth abundances in DSDP Sites 332, 334, and 335, and inferences on the Azores mantle blob activity with time. In Aumento, F., Melson, W. G., et al., *Init. Repts. DSDP*, 37: Washington (U.S. Govt. Printing Office), 591-597.
- Schilling, J.-G., and Noe-Nygaard, A., 1974. Faeroe-Iceland plume: rare-earth evidence. *Earth Planet. Sci. Lett.*, 24:1-14.
- Schilling, J.-G., and Ridley, W. I., 1975. Volcanic rocks from DSDP Leg 29: petrography and rare-earth abundances. In Kennett, J. P., Houtz, R. E., et al., *Init. Repts. DSDP*, 29: Washington (U.S. Govt. Printing Office), 1103-1107.
- Schilling, J.-G., Thompson, G., Kingsley, R., and Humphries, S., 1985. Hotspot-migrating ridge interactions in the South Atlantic. *Nature*, 313:187-191.
- Schilling, J.-G., Zajac, M., Evans, R., Johnston, T., White, W., Devine, J. D., and Kingsley, R., 1983. Petrological and geochemical variations along the Mid-Atlantic Ridge from 29°N to 73°N. *Am. J. Sci.*, 283:510-586.
- Verma, S. P., Schilling, J.-G., and Waggoner, D. G., 1983. Neodymium isotopic evidence for Galapagos hotspot-spreading centre system evolution. *Nature*, 306:654-657.
- Vogt, P. R., 1976. Plumes, sub-axial pipe flow, and topography along the mid-oceanic ridge. *Earth Planet. Sci. Lett.*, 29:309-325.
- Vogt, P. R., and Tucholke, B. E., 1979. The New England Seamounts: testing origins. In Tucholke, B. E., Vogt, P. R., et al., *Init. Repts. DSDP*, 43: Washington (U.S. Govt. Printing Office), 847-856.
- White, W. M., 1979. Geochemistry of basalts from the FAMOUS area: re-examination. *Carnegie Inst. Washington Year Book*, 78: 325-331.
- White, W. M., Bryan, W. B., 1977. Sr-isotope, K, Rb, Cs, Sr, Ba, and rare-earth geochemistry of basalts from the FAMOUS area. *Geol. Soc. Am. Bull.*, 88:571-576.
- White, W. M., and Schilling, J.-G., 1978. The nature and origin of geochemical variation in Mid-Atlantic Ridge basalts from the central North Atlantic. *Geochim. Cosmochim. Acta*, 42:1501-1516.
- Wood, D. A., 1979. Dynamic partial melting: its application to the petrogenesis of basalts erupted in Iceland, the Faeroe Island, the Isle of Skye (Scotland), and the Troodos Massif (Cyprus). *Geochim. Cosmochim. Acta*, 43:1031-1046.
- _____, 1981. Partial melting models for the petrogenesis of Reykjanes Peninsula basalts, Iceland: implications for the use of trace elements as strontium and neodymium isotope ratios to record in homogeneities in the upper mantle. *Earth Planet. Sci. Lett.*, 52: 183-190.
- Zindler, A., Hart, S. R., and Jakobsson, S. P., 1979. Nd and Sr isotope ratios and rare-earth element abundances in Reykjanes Peninsula basalts: evidence for mantle heterogeneity beneath Iceland. *Earth Planet. Sci. Lett.*, 45:249-262.

Date of Initial Receipt: 25 August 1983

Date of Acceptance: 4 April 1984